JACS
JOURNAL OF THE AMERICAN CHEMICAL SOCIETY

Communication

pubs.acs.org/JACS

Immobilizing Tetraphenylethylene into Fused Metallacycles: Shape Effects on Fluorescence Emission

Zhixuan Zhou,[†] Xuzhou Yan,[*,†,§] Manik Lal Saha,[*,†] Mingming Zhang,[†] Ming Wang,[‡,⊥] Xiaopeng Li,[‡] and Peter J. Stang[*,†]

[†]Department of Chemistry, University of Utah, 315 South 1400 East, Room 2020, Salt Lake City, Utah 84112, United States

[‡]Department of Chemistry and Biochemistry and Materials Science, Engineering, and Commercialization Program, Texas State University, San Marcos, Texas 78666, United States

Supporting Information

ABSTRACT: Herein, we describe the selective formation of a discrete fused metallarhomboid and a triangle by the careful control of the shape and stoichiometry of the building blocks. A tetraphenylethylene (TPE)-based tetrapyridyl donor is exploited as the bridging component, and coordination immobilization of the TPE unit within the rigid metallacyclic frameworks efficiently suppresses its intramolecular rotational motions. As a result, the fused polygons are innately emissive in dilute solution, representing an alternative to aggregation-induced emission. Upon further molecular aggregation, these metallacycles display aggregation-induced enhanced emissions. Interestingly, the fused rhomboid **7** shows a weaker fluorescence in dilute solutions relative to that of the fused triangle **8**, while a reversal of emission intensities was observed in the aggregated state. These markedly different fluorescence efficiencies are likely due to the differences in the shapes of the fused polygons. Thus, this work shows that the properties of supramolecular coordination complexes can be affected by subtle structural factors, which can be controlled easily and precisely at the molecular level.

Coordination-driven self-assembly is a powerful strategy for preparing supramolecular architectures due to the directional and predictable nature of the metal−ligand coordination interactions.[1] The kinetic reversibility of the self-assembly process between a Lewis-base-containing donor and a Lewis-acidic acceptor allows the system to undergo error correction and self-repairing processes, leading to the formation of a product that is thermodynamically favorable. These advantages enable the construction of a series of finite supramolecular coordination complexes (SCCs), including 2D polygons, 3D polyhedra, and other nanoscopic materials with pre-designed sizes and shapes, by controlling the size, geometry, and stoichiometry of the rigid precursors.[2] In addition, functional moieties can be introduced to the SCC scaffolds by the direct incorporation into the starting units, pendant attachment, or host−guest encapsulation.[3] For example, by the introduction of fluorophores into the SCC platforms, light-emitting SCCs have been constructed[4] which not only preserve the photophysical properties of the fluorophores but oftentimes provide new properties such as tunable emission wavelengths,[4b,e,f] markedly enhanced fluorescence efficiencies,[4g] and selective sensing.[4c,d]

Fluorescent materials have widespread applications in fields such as bioimaging, chemosensing, optoelectronics, etc.[5] As a result, the development of novel fluorophores has received continued interest. Conventional organic fluorophores often display weakened or even totally quenched emission in high concentrations or in the solid state due to the exciton interactions and non-radiative decays.[6] In contrast, aggregation-induced emission (AIE) refers to the phenomenon in which fluorophores are generally not emissive in dilute solutions but become highly emissive as aggregates.[7] AIE is attributed to the restriction of intramolecular motions of the twisted chromophores upon the formation of aggregates.[7]

Tetraphenylethylene (TPE) is an iconic and readily accessible AIE fluorophore in which phenyl ring rotation and ethylenic C═C bond twisting quench its fluorescence in dilute solutions.[8] Recent studies revealed that the formation of aggregates is not the only way to "*turn on*" the emission of TPEs, while other strategies, including covalent modifications,[9] embedding into metal−organic frameworks,[10] and non-covalent interactions such as host−guest interaction[11] and coordination,[4f,12] can be exploited to modulate their intramolecular motions. Molecular architectures consisting of TPE units have shown a wide variety of applications.[13] However, among these examples, formation of 3D cage-like architectures or extended polymeric networks is required in order to fully anchor the phenyl rings of the TPE units. Discrete 2D planar complexes with a TPE core have rarely been reported, although species with planar geometry may provide unique properties relative to non-planar ones in the preparation of materials.[14] In an effort to extend the scope of functional metal−organic materials based on SCC platforms, we herein describe the *de novo* design and synthesis of fused metallacyclic polygons **7** and **8** using a multicomponent self-assembly technique (Scheme 1) which has been used in the construction of other fused metallacyclic systems.[15]

As demonstrated in Scheme 1, a D_{4h}-symmetric TPE-based tetrapyridyl donor **2** is used as the bridging component of the fused metallacyclic polygons. In order to fit its connectivity, a 60° dipyridyl donor **1** and acceptors **3** and **4** were designed as the complementary precursors. Mixing **1** and **2** with a 120° di-Pt(II)

Received: July 11, 2016
Published: September 27, 2016

DOI: 10.1021/jacs.6b07173
J. Am. Chem. Soc. 2016, 138, 13131−13134

Scheme 1. Syntheses of Rhomboid 5, Triangle 6, Double Rhomboid 7, and Double Triangle 8 via Multicomponent Coordination-Driven Self-Assembly

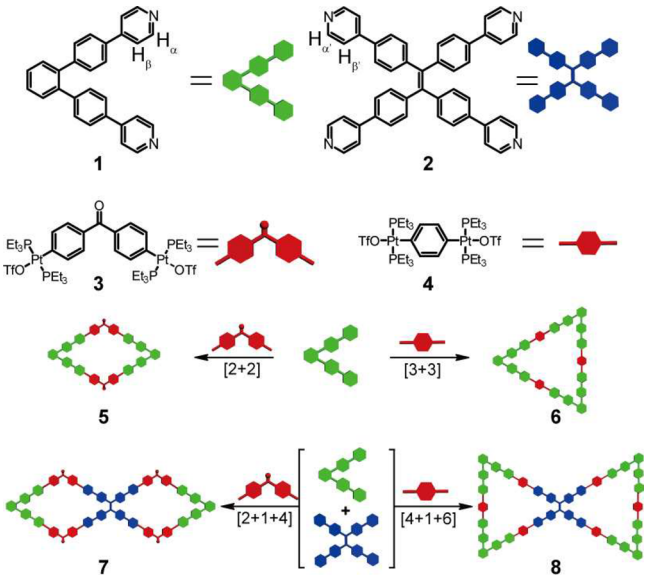

acceptor **3** in a 2:1:4 ratio allows the formation of double rhomboid **7** via coordination-driven self-assembly, whereas double triangle **8** was selectively formed from a 4:1:6 mixture of ligands **1**, **2**, and a 180° di-Pt(II) acceptor **4**. In dilute solutions, these fused polygons are emissive owing to the formation of metal−ligand bonds that hinder the intramolecular rotations of the TPE core. Further emission enhancements were observed in their aggregated states, due to tight molecular packing. The photophysical properties of these polygons vary due to differences in their shapes and framework rigidity, which can be controlled at the molecular level by changing the precursor building blocks. These features, along with good processability of SCCs,[4b] demonstrate the potential of this approach for the facile construction of functional materials.

Stirring a mixture of donors **1** and **2** and the acceptors in appropriate ratios in CH_2Cl_2/acetone (1:1, v/v) at room temperature led to the formation of [2+1+4] double rhomboid **7** or [4+1+6] double triangle **8** in nearly quantitative yields (Scheme 1). Likewise, the model [2+2] rhomboid **5** and the [3+3] triangle **6** were synthesized by mixing donor **1** with acceptors **3** and **4**, respectively, in an appropriate stoichiometry. These products were isolated by precipitation with diethyl ether, dried, and re-dissolved in DMSO-d_6 for characterization.

^{1}H and ^{31}P NMR analysis of compounds **5**−**8** indicated the formation of discrete assemblies with high symmetry. For simple polygons **5** and **6**, sharp singlets were observed in the $^{31}P\{^1H\}$ NMR spectra (SI, Figures S4 and S7), as expected. However, each of the fused polygons shows overlapping signals with concomitant ^{195}Pt satellites in its $^{31}P\{^1H\}$ NMR spectrum, even at elevated temperatures (SI, Figures S10 and S13). This suggests that the chemical environment around the P atoms varies little due to the similarity in size and geometry between the two types of donors.[15] In the ^{1}H NMR spectra of these assemblies (Figure 1, and SI, Figures S3, S6, S9, and S12), signals corresponding to the pyridyl units exhibited downfield shifts relative to those of the free donor building blocks ($\Delta\delta \approx 0.15$ and 0.40 ppm for α- and β-pyridyl protons, respectively), suggesting that the formation of metal−ligand coordination bonds causes a loss of the electron density of the pyridyl units. Electrospray ionization time-of-flight

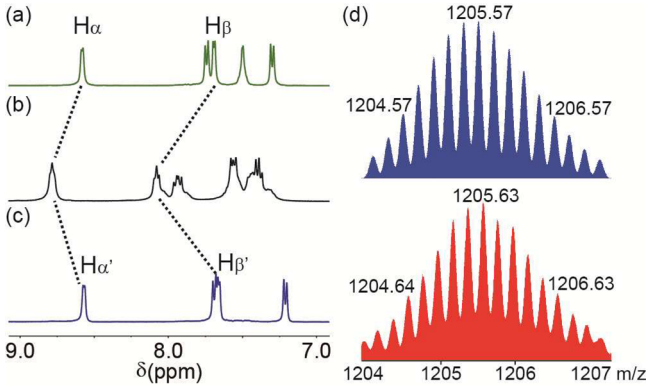

Figure 1. (a−c) Partial ^{1}H NMR spectra (500 MHz, DMSO-d_6, 298 K) of **1** (a), double rhomboid **7** (b), and donor **2** (c). (d) Experimental (red) and calculated (blue) ESI-TOF-MS spectra of **7** $[M - 5OTf]^{5+}$.

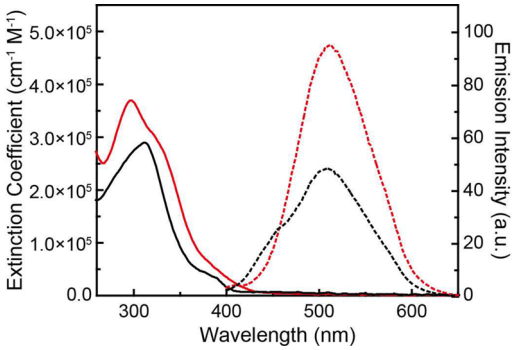

Figure 2. Absorption (solid) and emission (dashed) profiles for **7** (black) and **8** (red) in CH_2Cl_2 (λ_{ex} = 345 nm, c = 4.00 μM).

mass spectrometry (ESI-TOF-MS) was employed to demonstrate the stoichiometry of the metallacycles. Isotopically resolved peaks corresponded to an intact entity with charge states arising from the loss of trifluoromethanesulfonate (OTf) counterions were identified for each assembly. For example, peaks at m/z (Da) = 1576.47, 2282.64, 1205.63, and 1770.47, corresponding to $[M - 2OTf]^{2+}$, $[M - 2OTf]^{2+}$, $[M - 5OTf]^{5+}$, and $[M-5OTf]^{5+}$ for **5**−**8**, respectively, support their stoichiometry as shown in Scheme 1. Moreover, the quantitative formation of the polygons was confirmed via diffusion-ordered ^{1}H NMR spectroscopy (DOSY) experiments, which show a single vertical trace in all cases (SI, Figures S15−S18). The measured diffusion coefficients for **7** and **8** are 4.01×10^{-11} and 3.59×10^{-11} $m^2 \cdot s^{-1}$, respectively. These values are smaller than those for the corresponding model rhomboid **5** (6.60×10^{-11} $m^2 \cdot s^{-1}$) and triangle **6** (8.13×10^{-11} $m^2 \cdot s^{-1}$), further suggesting that the Stokes−Einstein hydrodynamic radii of the fused assmblies are roughly double in values as compared to their corrosponding simple counterparts, as also expected from their geometry. Moreover, these experimental values are in good agreement with those obtained by PM6/DFT molecular stimulations (SI, Figures S31 and S32).

The absorption and emission profiles for the fused metallacycles in CH_2Cl_2 are shown in Figure 2. Both **7** and **8** display a broad absorption band centered at ca. 300 nm due to the presence of donors and acceptors with π-conjugated systems. Notably, the double triangle **8** exhibits a shoulder at 345 nm, which is likely due to absorption from the donor **2**. This is because at the same wavelength, no peak is observed for the model triangle **6** under identical conditions. However, for the

DOI: 10.1021/jacs.6b07173
J. Am. Chem. Soc. 2016, 138, 13131−13134

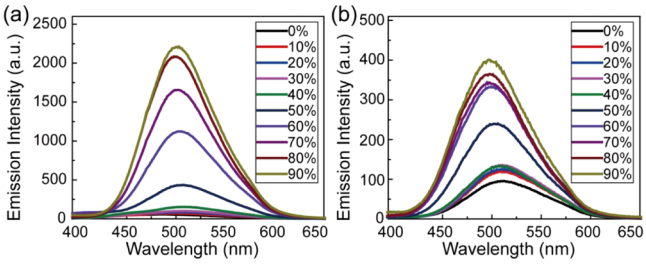

Figure 3. Fluorescence emission spectra of **7** (a) and **8** (b) versus hexane fraction in CH_2Cl_2/hexane mixtures (λ_{ex} = 345 nm, c = 4.00 μM).

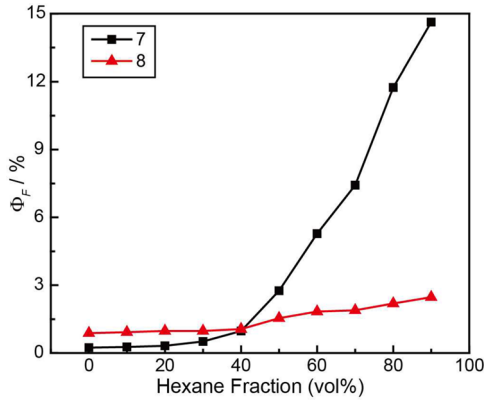

Figure 4. Quantum yields of **7** and **8** versus hexane fraction in CH_2Cl_2/hexane mixtures, determined using quinine sulfate at 365 nm (Φ_F = 56.0%).

double rhomboid **7**, the absorption band(s) of the donor **2** are merged. In their fluorescence spectra, an emission band centered at ca. 510 nm is observed. Since the ligand **1**, Pt precursors, and simple rhomboid **5** and triangle **6** are not emissive under these conditions (SI, Figures S23–S28), these emissions are likely due to the TPE units. This suggests that the intramolecular motions of the TPE moieties are inhibited upon incorporation into the rigid metallacyclic frameworks, which suppressed the non-radiative decay process and thus turned on these emissions. However, the presence of platinum centers may cause an emission quenching, due to their heavy atom effects.[17] Notably, under the same conditions, double rhomboid **7** displayed weaker emission intensity relative to that of the double triangle **8**, even though both contain a single TPE fluorophore and the latter has higher numbers of Pt centers relative to the former.

To gain further insight into the light-emitting behavior of these assemblies, the fluorescence spectra were recorded in CH_2Cl_2/hexane mixtures (Figure 3). Introduction of hexane into the CH_2Cl_2 solutions reduces the solubility of the assemblies and thereby facilitates aggregate formation. With a constant increase of the hexane content, the fluorescence intensities were chronologically increased and reached a maximum at 90% hexane content. This is consistent with the expected AIE behavior and indicative of a further suppression of the intramolecular motions of the embedded TPE units upon aggregation. Interestingly, in the aggregated states (hexane content = 90%), a 45-fold fluorescence enhancement is observed for **7**, whereas **8** displayed only a 4.2-fold fluorescence enhancement. As a result, the double rhomboid **7** showed a higher fluorescence intensity relative to double triangle **8** in the aggregated states, which is exactly opposite to what was observed in dilute solutions. In addition, a slight blue shift (ca. 5 nm) of the emission maximum was observed for each case (Figure 3), which is attributed to the charge-transfer (CT) process within the assemblies. The CT process is known to red shift the emission of AIE fluorophores in polar solution, and it is attenuated in a less polar environment.[4f] Introduction of hexane results in the decrease in the polarity of the solution, thereby causing a blue shift.

The AIE characteristics of these polygons in mixed solutions were further probed by changes in quantum yields (Φ_F). In CH_2Cl_2, they exhibited relatively low Φ_F values of 0.24% and 0.88% for **7** and **8**, respectively. With an increase in hexane content, marked increases in the Φ_F values were observed. At a 90% hexane fraction, their Φ_F values reached 14.6% and 2.5%, respectively (Figure 4). This trend is consistent with the fluorescence enhancement of the assemblies.

The sharp difference in the light-emitting behavior between the double rhomboid and the double triangle, as shown in their emission intensities and Φ_F enhancements, implies that the shape of the assemblies exerts considerable influence on their light-emitting properties. Triangles are known to provide strength and rigidity to structures, and these characteristics have been extensively exploited by both nature and scientists in the construction of stable architectures.[17] Hence, we anticipated that, in dilute solution, the immobilization of the TPE moiety within a double triangular structure imposes more restrictions on its intramolecular motions than immobilization in a double rhomboidal structure. To substantiate this hypothesis, PM6 computations were performed to calculate the activation barrier for ring flipping of the TPE moiety within the assemblies **7** and **8**. The calculated activation barrier for double rhomboid **7** is lower than that of double triangle **8** by 4.3 kJ/mol (SI, Figure S33). Since the inhibition of the TPE phenyl ring motions plays a key role in inducing emission of these assemblies,[8] the higher activation barrier for the double triangle is consistent with its higher fluorescence intensities and Φ_F value relative to those of the double rhomboid in dilute solution. In the aggregated state, for both double rhomboid and double triangle, the intramolecular motions were fully inhibited by tight packing of the TPE units. The lower fluorescence intensity and quantum yield of the double triangle **8** relative to those of double rhomboid **7** are likely because of two reasons: (1) The relative flexibility of the rhomboidal skeletons may allow them to aggregate much more tightly than the rigid triangular structures, as observed in dynamic light-scattering measurements (SI, Figures S29 and S30). Under identical conditions, **7** forms larger aggregates than **8** ($\Delta d_h \approx 30$ nm; d_h is the diameter). (2) The double triangle **8** contains a higher number of Pt centers than **7**, which may increase the intersystem crossing and thus lower its emission.[16]

The solvent effects on the emission profiles were also examined. Because of the CT processes within the assemblies, increasing the polarity of the solvent results in a red shift in the emission maximum of each solution of the assemblies. However, there was little effect (<15 nm) on the emission maximum for the emission profiles. As an example, the absorption and emission profiles for **8** in different solvents can be found in SI, Figures S21 and S22.

In conclusion, we present the synthesis of TPE-core fused metallacyclic polygons by the stoichiometric and structural control of the multicomponent mixtures of different pyridyl donors and platinum acceptors. The intramolecular motions of the TPE-based tetrapyridyl unit are anchored within the supramolecular ensembles by the dative bonds, and they can be further inhibited by molecular packing upon aggregation. As a

DOI: 10.1021/jacs.6b07173
J. Am. Chem. Soc. 2016, 138, 13131–13134

result, the assemblies exhibit fluorescence emissions both in dilute solutions and in the aggregated state, which may be used for the fabrication of optoelectronic materials with multifaceted functionality. Moreover, due to the differences in the strength and rigidity of the assemblies, as imposed by their shapes, different fluorescence enhancement behaviors are observed for the double rhomboid and double triangle. This phenomenon demonstrates that the properties of SCCs could be greatly influenced by their geometries. This characteristic, combined with the versatility, high efficiency, and good modularity of coordination self-assembly, suggests that coordination-driven self-assembly can serve as the basis for the bottom-up synthesis of materials whose functions are readily tunable by controlling the geometry and stoichiometry of precursors and may enable various applications such as probing/sensing, selective absorption/removal, and targeted delivery.

■ ASSOCIATED CONTENT

Supporting Information

The Supporting Information is available free of charge on the ACS Publications website at DOI: 10.1021/jacs.6b07173.

Experimental details and additional data (PDF)

■ AUTHOR INFORMATION

Corresponding Authors

*xzyan@stanford.edu
*manik.saha@utah.edu
*stang@chem.utah.edu

Present Addresses

§X.Y.: Department of Chemical Engineering, Stanford University, Stanford, California 94305, United States
⊥M.W.: State Key Laboratory of Supramolecular Structure and Materials, College of Chemistry, Jilin University, Changchun, Jilin 130012, P. R. China

Notes

The authors declare no competing financial interest.

■ ACKNOWLEDGMENTS

P.J.S. thanks the NSF (Grant 1212799) for financial support. X.L. thanks the NSF (CHE-1506722) and PREM Center of Texas State University (DMR-1205670) for financial support. Computational resources are gratefully acknowledged from the Center for High Performance Computing (CHPC) at the University of Utah.

■ REFERENCES

(1) (a) Leininger, S.; Olenyuk, B.; Stang, P. J. *Chem. Rev.* **2000**, *100*, 853. (b) Fujita, M.; Tominaga, M.; Hori, A.; Therrien, B. *Acc. Chem. Res.* **2005**, *38*, 369. (c) Oliveri, C. G.; Ulmann, P. A.; Wiester, M. J.; Mirkin, C. A. *Acc. Chem. Res.* **2008**, *41*, 1618. (d) Ward, M. D. *Chem. Commun.* **2009**, 4487. (e) Han, M.; Engelhard, D. M.; Clever, G. H. *Chem. Soc. Rev.* **2014**, *43*, 1848. (f) Castilla, A. M.; Ramsay, W. J.; Nitschke, J. R. *Acc. Chem. Res.* **2014**, *47*, 2063. (g) Mukherjee, S.; Mukherjee, P. S. *Chem. Commun.* **2014**, *50*, 2239. (h) Saha, M. L.; Neogi, S.; Schmittel, M. *Dalton Trans.* **2014**, *43*, 3815. (i) Cook, T. R.; Stang, P. J. *Chem. Rev.* **2015**, *115*, 7001. (j) Brown, C. J.; Toste, F. D.; Bergman, R. G.; Raymond, K. N. *Chem. Rev.* **2015**, *115*, 3012. (k) Newkome, G. R.; Moorefield, C. N. *Chem. Soc. Rev.* **2015**, *44*, 3954.

(2) (a) Stang, P. J.; Olenyuk, B. *Acc. Chem. Res.* **1997**, *30*, 502. (b) Chakrabarty, R.; Mukherjee, P. S.; Stang, P. J. *Chem. Rev.* **2011**, *111*, 6810.

(3) (a) Therrien, B.; Süss-Fink, G.; Govindaswamy, P.; Renfrew, A. K.; Dyson, P. J. *Angew. Chem., Int. Ed.* **2008**, *47*, 3773. (b) Cook, T. R.; Vajpayee, V.; Lee, M. H.; Stang, P. J.; Chi, K.-W. *Acc. Chem. Res.* **2013**, *46*, 2464. (c) Yoshizawa, M.; Klosterman, J. K. *Chem. Soc. Rev.* **2014**, *43*, 1885. (d) Browne, C.; Ramsay, W. J.; Ronson, T. K.; Medley-Hallam, J.; Nitschke, J. R. *Angew. Chem., Int. Ed.* **2015**, *54*, 11122. (e) Zhukhovitskiy, A. V.; Zhong, M.; Keeler, E. G.; Michaelis, V. K.; Sun, J. E. P.; Hore, M. J. A.; Pochan, D. J.; Griffin, R. G.; Willard, A. P.; Johnson, J. A. *Nat. Chem.* **2015**, *8*, 33. (f) Xu, L.; Wang, Y.-X.; Chen, L.-J.; Yang, H.-B. *Chem. Soc. Rev.* **2015**, *44*, 2148. (g) Howlader, P.; Das, P.; Zangrando, E.; Mukherjee, P. S. *J. Am. Chem. Soc.* **2016**, *138*, 1668. (h) Wang, Q. Q.; Gonell, S.; Leenders, S. H.; Durr, M.; Ivanovic-Burmazovic, I.; Reek, J. N. *Nat. Chem.* **2016**, *8*, 225. (i) Jiang, B.; Zhang, J.; Ma, J.-Q.; Zheng, W.; Chen, L.-J.; Sun, B.; Li, C.; Hu, B.-W.; Tan, H.; Li, X.; Yang, H.-B. *J. Am. Chem. Soc.* **2016**, *138*, 738. (j) Zhou, Z.; Yan, X.; Cook, T. R.; Saha, M. L.; Stang, P. J. *J. Am. Chem. Soc.* **2016**, *138*, 806.

(4) (a) Kaloudi-Chantzea, A.; Karakostas, N.; Raptopoulou, C. P.; Psycharis, V.; Saridakis, E.; Griebel, J.; Hermann, R.; Pistolis, G. *J. Am. Chem. Soc.* **2010**, *132*, 16327. (b) Pollock, J. B.; Schneider, G. L.; Cook, T. R.; Davies, A. S.; Stang, P. J. *J. Am. Chem. Soc.* **2013**, *135*, 13676. (c) Neelakandan, P. P.; Jiménez, A.; Nitschke, J. R. *Chem. Sci.* **2014**, *5*, 908. (d) Shanmugaraju, S.; Mukherjee, P. S. *Chem. - Eur. J.* **2015**, *21*, 6656. (e) Yamashina, M.; Sartin, M. M.; Sei, Y.; Akita, M.; Takeuchi, S.; Tahara, T.; Yoshizawa, M. *J. Am. Chem. Soc.* **2015**, *137*, 9266. (f) Yan, X.; Cook, T. R.; Wang, P.; Huang, F.; Stang, P. J. *Nat. Chem.* **2015**, *7*, 342. (g) Yan, X.; Wang, M.; Cook, T. R.; Zhang, M.; Saha, M. L.; Zhou, Z.; Li, X.; Huang, F.; Stang, P. J. *J. Am. Chem. Soc.* **2016**, *138*, 4580.

(5) Valeur, B.; Berberan-Santos, M. N. *Molecular fluorescence: principles and applications*; John Wiley & Sons: New York, 2012.

(6) (a) Birks, J. B. *Photophysics of Aromatic Molecules*; Wiley: London, 1970. (b) Tang, C. W.; VanSlyke, S. A. *Appl. Phys. Lett.* **1987**, *51*, 913.

(7) Mei, J.; Leung, N. L.; Kwok, R. T.; Lam, J. W.; Tang, B. Z. *Chem. Rev.* **2015**, *115*, 11718.

(8) Dong, Y.; Lam, J. W. Y.; Qin, A.; Liu, J.; Li, Z.; Tang, B. Z.; Sun, J.; Kwok, H. S. *Appl. Phys. Lett.* **2007**, *91*, 011111.

(9) Shi, J.; Chang, N.; Li, C.; Mei, J.; Deng, C.; Luo, X.; Liu, Z.; Bo, Z.; Dong, Y. Q.; Tang, B. Z. *Chem. Commun.* **2012**, *48*, 10675.

(10) (a) Shustova, N. B.; McCarthy, B. D.; Dincă, M. *J. Am. Chem. Soc.* **2011**, *133*, 20126. (b) Wei, Z.; Gu, Z.-Y.; Arvapally, R. K.; Chen, Y.-P.; McDougald, R. N.; Ivy, J. F.; Yakovenko, A. A.; Feng, D.; Omary, M. A.; Zhou, H.-C. *J. Am. Chem. Soc.* **2014**, *136*, 8269.

(11) (a) Liang, G.; Lam, J. W. Y.; Qin, W.; Li, J.; Xie, N.; Tang, B. Z. *Chem. Commun.* **2014**, *50*, 1725. (b) Wu, J.; Sun, S.; Feng, X.; Shi, J.; Hu, X.-Y.; Wang, L. *Chem. Commun.* **2014**, *50*, 9122.

(12) (a) Zhao, J.; Yang, D.; Zhao, Y.; Yang, X. J.; Wang, Y. Y.; Wu, B. *Angew. Chem., Int. Ed.* **2014**, *53*, 6632. (b) Yan, X.; Wang, H.; Hauke, C. E.; Cook, T. R.; Wang, M.; Saha, M. L.; Zhou, Z.; Zhang, M.; Li, X.; Huang, F.; Stang, P. J. *J. Am. Chem. Soc.* **2015**, *137*, 15276.

(13) (a) Shustova, N. B.; Cozzolino, A. F.; Reineke, S.; Baldo, M.; Dincă, M. *J. Am. Chem. Soc.* **2013**, *135*, 13326. (b) Zhang, M.; Feng, G.; Song, Z.; Zhou, Y.-P.; Chao, H.-Y.; Yuan, D.; Tan, T. T. Y.; Guo, Z.; Hu, Z.; Tang, B. Z.; Liu, B.; Zhao, D. *J. Am. Chem. Soc.* **2014**, *136*, 7241. (c) Chen, L.-J.; Ren, Y.-Y.; Wu, N.-W.; Sun, B.; Ma, J.-Q.; Zhang, L.; Tan, H.; Liu, M.; Li, X.; Yang, H.-B. *J. Am. Chem. Soc.* **2015**, *137*, 11725. (d) Fan, W.-J.; Sun, B.; Ma, J.; Li, X.; Tan, H.; Xu, L. *Chem. - Eur. J.* **2015**, *21*, 12947. (e) Chowdhury, A.; Howlader, P.; Mukherjee, P. S. *Chem. - Eur. J.* **2016**, *22*, 7468. (f) Tian, Y.; Yan, X.; Saha, M. L.; Niu, Z.; Stang, P. J. *J. Am. Chem. Soc.* **2016**, *138*, 12033.

(14) (a) Williams, M. E.; Benkstein, K. D.; Abel, C.; Dinolfo, P. H.; Hupp, J. T. *Proc. Natl. Acad. Sci. U. S. A.* **2002**, *99*, 5171. (b) Hu, J.; Li, Y.; Ji, Z.; Jiang, G.; Yang, L.; Hu, W.; Gao, H.; Jiang, L.; Wen, Y.; Song, Y.; Zhu, D. *J. Mater. Chem.* **2007**, *17*, 3530. (c) Yokoyama, D. *J. Mater. Chem.* **2011**, *21*, 19187.

(15) Lee, J.; Ghosh, K.; Stang, P. J. *J. Am. Chem. Soc.* **2009**, *131*, 12028.

(16) Pollock, J. B.; Schneider, G. L.; Cook, T. R.; Davies, A. S.; Stang, P. J. *J. Am. Chem. Soc.* **2013**, *135*, 13676.

(17) Keten, S.; Xu, Z.; Buehler, M. J. *Mater. Sci. Eng., C* **2011**, *31*, 775.

DOI: 10.1021/jacs.6b07173
J. Am. Chem. Soc. 2016, 138, 13131−13134